

Original Article



# **<sup>18</sup>F-THK5351 PET Imaging in the Behavioral Variant of Frontotemporal Dementia**

## OPEN ACCESS

**Received:** Dec 9, 2018

**Revised:** Dec 25, 2018

**Accepted:** Dec 31, 2018

### **Correspondence to**

**Young Noh, MD**

Department of Neurology, Gachon University Gil Medical Center, Gachon University College of Medicine, 21 Namdong-daero 774-gil, Namdong-gu, Incheon 21565, Korea.

E-mail: ynoh@gachon.ac.kr

**Dong Jin Shin, MD**

Department of Neurology, Gachon University Gil Medical Center, Gachon University College of Medicine, 21 Namdong-daero 774-gil, Namdong-gu, Incheon 21565, Korea.  
E-mail: djshin@gilhospital.com

\*Gijin Nam and Hye Jin Jeong contributed equally to this work.

© 2018 Korean Dementia Association  
This is an Open Access article distributed under the terms of the Creative Commons Attribution Non-Commercial License (<https://creativecommons.org/licenses/by-nc/4.0/>) which permits unrestricted non-commercial use, distribution, and reproduction in any medium, provided the original work is properly cited.

### **ORCID iDs**

Gijin Nam

<https://orcid.org/0000-0003-4876-2904>

Hye Jin Jeong

<https://orcid.org/0000-0003-3765-8546>

Jae Myeong Kang

<https://orcid.org/0000-0003-0803-9332>

Sang-Yoon Lee

<https://orcid.org/0000-0002-6029-8553>

Seongho Seo

<https://orcid.org/0001-7894-0535>

**Gijin Nam ,<sup>1,\*</sup> Hye Jin Jeong ,<sup>2,\*</sup> Jae Myeong Kang ,<sup>3</sup> Sang-Yoon Lee ,<sup>4</sup> Seongho Seo ,<sup>3</sup> Ha-Eun Seo ,<sup>2</sup> Kee Hyung Park ,<sup>5</sup> Byeong Kil Yeon ,<sup>3</sup> Tatsuo Ido ,<sup>2</sup> Dong Jin Shin ,<sup>5</sup> Young Noh ,<sup>5,6</sup>**

<sup>1</sup>College of Medicine, Gachon University, Incheon, Korea

<sup>2</sup>Neuroscience Research Institute, Gachon University, Incheon, Korea

<sup>3</sup>Department of Psychiatry, Gachon University Gil Medical Center, Gachon University College of Medicine, Incheon, Korea

<sup>4</sup>Department of Neuroscience, Gachon University College of Medicine, Incheon, Korea

<sup>5</sup>Department of Neurology, Gachon University Gil Medical Center, Gachon University College of Medicine, Incheon, Korea

<sup>6</sup>Department of Health Science and Technology, Gachon Advanced Institute for Health Sciences & Technology, Gachon University, Incheon, Korea

## **ABSTRACT**

**Background and Purpose:** Behavioral variant frontotemporal dementia (bvFTD) is a subtype of frontotemporal dementia, which has clinical symptoms of progressive personality and behavioral changes with deterioration of social cognition and executive functions. The pathology of bvFTD is known to be tauopathy or TDP-43 equally. We analyzed the <sup>18</sup>F-THK5351 positron emission tomography (PET) scans, which were recently developed tau PET, in patients with clinically-diagnosed bvFTD.

**Methods:** Forty-eight participants, including participants with behavioral variant frontotemporal dementia (bvFTD, n=3), Alzheimer's disease (AD, n=21) and normal cognition (NC, n=24) who completed 3T magnetic resonance images, <sup>18</sup>F-THK5351 PET scans, and detailed neuropsychological tests were included in the study. Voxel-wise statistical analysis and region of interest (ROI)-based analyses were performed to evaluate the retention of THK in bvFTD patients.

**Results:** In the voxel-based and ROI-based analyses, patients with bvFTD showed greater THK retention in the prefrontal, medial frontal, orbitofrontal, anterior cingulate, insula, anterior inferior temporal and striatum regions compared to NC participants. Left-right asymmetry was noted in the bvFTD patients. A patient with extrapyramidal symptoms showed much greater THK retention in the brainstem.

**Conclusions:** The distribution of THK retention in the bvFTD patients was mainly in the frontal, insula, anterior temporal, and striatum regions which are known to be the brain regions corresponding to the clinical symptoms of bvFTD. Our study suggests that <sup>18</sup>F-THK5351 PET imaging could be a supportive tool for diagnosis of bvFTD.

**Keywords:** Frontotemporal Dementia; Tauopathies; Positron-Emission Tomography

Ha-Eun Seo  <https://orcid.org/0000-0003-4452-0908>  
 Kee Hyung Park  <https://orcid.org/0000-0001-6847-6679>  
 Byeong Kil Yeo  <https://orcid.org/0000-0002-4853-3178>  
 Tatsuo Ido  <https://orcid.org/0000-0002-2825-9343>  
 Dong Jin Shin  <https://orcid.org/0000-0003-4346-4000>  
 Young Noh  <https://orcid.org/0000-0002-9633-3314>

#### Funding

This study was supported by a grant (HI14C1135) of the Korea Healthcare Technology R&D Project through the Korea Health Industry Development Institute (KHIDI) funded by the Ministry of Health & Welfare, Republic of Korea.

#### Conflict of Interest

The authors have no financial conflicts of interest.

#### Author Contributions

Conceptualization: Ido T, Noh Y. Data curation: Jeong HJ, Kang JM, Lee SY, Seo S, Park KH, Yeon BK, Ido T, Shin DJ, Noh Y. Formal analysis: Nam G, Jeong HJ, Seo S. Funding acquisition: Noh Y. Investigation: Jeong HJ, Kang JM, Lee SY, Noh Y. Methodology: Jeong HJ, Seo S, Seo HE, Noh Y. Project administration: Noh Y. Resources: Jeong HJ, Lee SY, Noh Y. Software: Seo S. Supervision: Noh Y. Validation: Lee SY, Seo S, Park KH, Yeon BK, Shin DJ. Visualization: Jeong HJ, Seo S. Writing - original draft: Nam G, Jeong HJ. Writing - review & editing: Kang JM, Seo HE, Ido T, Shin DJ, Noh Y.

## INTRODUCTION

Frontotemporal dementia (FTD) is a family of disorders representing tau aggregates which are also present in the pathology of Pick's disease, corticobasal degeneration (CBD), and progressive supranuclear palsy (PSP). The most common subtype of FTD is the behavioral variant frontotemporal dementia (bvFTD), which presents with progressive personality and behavioral changes with deterioration of social cognition and executive functions. The pathology of bvFTD has been known to be heterogeneous with variable molecular components, including tau (FTLD-tau), TDP-43 (FTLD-TDP), fused in sarcoma proteins (FTLD-FUS), ubiquitin-proteasome system (FTLD-UPS), and neuronal intermediate filaments (FTLD-ni).<sup>1</sup> About 50% of the main pathologies of bvFTD are known to be comprised of tauopathy.<sup>2-4</sup>

Although the most common molecular pathology is tau protein, which is highly correlated with frontotemporal lobar degeneration, many bvFTD patients have multiple overlapped neuropathologies.<sup>5</sup> Tau protein has different isoforms, three repeats (3R) in Pick's disease, and 4 repeats (4R) in CBD and PSP.<sup>6</sup> Aggregation of tau leads to the formation of neurotoxic neurofibrillary tangles which disrupt normal neuronal function and cause neuronal death.<sup>7</sup> Since tauopathy is correlated with disease severity and its distribution is related to symptoms in bvFTD, tau can be a useful biomarker of bvFTD. <sup>18</sup>F-THK5351 is a positron emission tomography (PET) tracer targeting tau deposits used to assess neurofibrillary tangles *in vivo*.<sup>7,8</sup> <sup>18</sup>F-THK5351 was developed to reduce non-specific retention in the subcortical white matter compared to previous tau tracers. <sup>18</sup>F-THK5351 has a high signal-to-background ratio and off-target binding in basal ganglia with no remarkable retention in the choroid plexus or venous sinus, which can cause spill-in of the tracer signals into the brain.<sup>8</sup> Moreover, its non-specific binding in non-tau pathologies can help to assess neurodegeneration. Although many similar tau PET tracers, such as <sup>18</sup>F-flortaucipir, were developed as tools for the *in vivo* assessment of tauopathy, tracers found in the cortical or subcortical regions did not correlate with the severity of cognitive dysfunction and the tracers displayed widespread off-target binding in the white matter and basal ganglia.<sup>9</sup> However, <sup>18</sup>F-THK5351 is a quinolone-derived agent, which can bind normal monoamine oxidase B (MAO-B) in the basal ganglia<sup>10</sup> and that from reactive astrocytes in neuroinflammatory states.<sup>11</sup>

In this study, we analyzed the <sup>18</sup>F-THK5351 PET scans of patients with clinically-diagnosed bvFTD presenting with obvious changes in behavior and personality. The regional pattern of THK retention in bvFTD patients was compared with normal cognition (NC) and Alzheimer's disease (AD) patients.

## METHODS

### Participants

Forty-eight participants, including participants with bvFTD ( $n=3$ ), AD ( $n=21$ ), and NC ( $n=24$ ) who completed 3T magnetic resonance images (MRIs), <sup>18</sup>F-THK5351 PET scans, and detailed neuropsychological tests were included. Three bvFTD patients were classified using the criteria stipulated by the International bvFTD Criteria Consortium.<sup>12</sup> AD patients diagnosed according to the National Institute of Neurological and Communicative Disorders and Stroke and the Alzheimer's Disease and Related Disorders Association (NINCDS-ADRDA)<sup>13</sup> criteria were included in the study. In the NC group, the Clinical Dementia Rating (CDR) scores were

zero, the Mini-Mental Status Examination (MMSE) scores were above 25, and the overall neuropsychological test performances were 1.5 standard deviations above the age- and education-adjusted norms.

This study was approved by the Institutional Review Board (IRB) of Gachon Medical Center (IRB No. GDIRB2015-272) and written informed consent was obtained from all participants.

### **Neuropsychological test**

All participants underwent a neuropsychological evaluation using a battery of tests that included assessments for the following cognitive domains: attention, language, praxis, visuo-constructive ability, elements of Gerstmann syndrome, visual and verbal memory, and frontal/executive function. Quantifiable tests included the digit span test (forward and backward); the Rey-Osterrieth Complex Figure Test; the Korean version of the Boston Naming Test; the Seoul Verbal Learning Test; the contrasting program; the Go/No Go test; the phonemic, animal, and supermarket Controlled Oral Word Association Test; the Trail Making Test-A and -B; and a Stroop Test (color and word reading of 112 items during a 2-min period). Results from the MMSE, CDR, CDR Sum of Boxes, and the Geriatric Depression Scale were also obtained. The neuropsychiatric inventory (NPI) score was obtained by multiplication of the severity and frequency of each item to evaluate noncognitive behavioral and psychiatric disturbances, including delusions, hallucinations, aggression, depression, anxiety, euphoria, apathy, disinhibition, irritability, abnormal repetitive behaviors, night-time behavior, and eating changes.<sup>14</sup>

### **Image acquisition and preprocessing**

#### *MRI acquisition*

MRI of all participants was performed on a 3.0T MRI scanner (Verio, Siemens with a Siemens matrix coil) and included a 3D T1 magnetization-prepared rapid gradient-echo (MPRAGE) sequence. The 3D T1-MPRAGE imaging parameters used were as follows: repetition time=1,900 m/s, echo time=2.93 m/s, flip angle=8°, pixel bandwidth=170 Hz/pixel, matrix size=256×208, field of view=256 mm, total acquisition time=4 minutes 10 seconds, and an iso-voxel resolution of 1.0 mm.

#### *PET acquisition*

All subjects underwent PET scans using <sup>18</sup>F-THK5351. Amyloid β imaging PET scans using <sup>18</sup>F-flutemetamol (FLUTE) were obtained in three bvFTD patients. All PET scans were obtained using a Siemens Biograph 6 Truepoint PET/computed tomography (CT) scanner (Siemens, Knoxville, TN, USA) with a list-mode emission acquisition. All subjects underwent a 20-minute emission scan 90 minutes after the intravenous injection of 185 MBq of <sup>18</sup>F-FLUTE. Within three months of undergoing the initial FLUTE PET scans, all participants underwent a 20-minute emission scan 50 minutes after the intravenous injection of 185 MBq of <sup>18</sup>F-THK5351. A low-dose CT was performed for attenuation correction prior to all scans. The images were reconstructed in a 256×256×109 matrix with a voxel size of 1.33×1.33×1.5 mm using a 2D ordered subset expectation maximization algorithm (8 iterations, 16 subsets) and were corrected for physical effects, including radiation attenuation and scatter.

#### *Image processing and analysis*

Individual PET data were co-registered to 3D T1-MPRAGE images using FreeSurfer (Martinos Center for Biomedical Imaging, Charlestown, MA, USA). The regional mean values of the PET images were then extracted after region-based partial volume correction using the PETSurfer

tool in FreeSurfer.<sup>15,16</sup> In order to compare the THK retention in each group quantitatively, we defined 25 regions of interest (ROIs), including the frontal cortex (the superior and middle frontal gyrus; the orbital part of the superior, middle, and inferior orbital frontal gyrus; the opercular part of the inferior frontal gyrus; and the triangular part of the inferior frontal gyrus), lateral temporal cortex (superior, middle, and inferior temporal cortex), superior parietal cortex, inferior parietal cortex (inferior parietal, supramarginal gyrus, and angular gyrus), occipital cortex (superior, middle, and inferior occipital gyrus, and cuneus), anterior cingulate gyrus, posterior cingulate gyrus, mesial temporal cortex (hippocampus, parahippocampal gyrus, and amygdala), striatum (putamen and pallidum), fusiform gyrus, inferior temporal cortex, and temporal pole. The subject's mean THK standardized uptake value ratio (SUVR) for the frontal, lateral temporal, superior and inferior parietal, and precuneus-posterior cingulate cortices (PC-PCC) were used to determine the global tau burden. The THK retention was expressed as an SUVR using the cerebellar gray matter as the reference region,<sup>17,19</sup> and FLUTE retention was also expressed as an SUVR using the pons as the reference region.<sup>20</sup> Amyloid PET imaging was considered negative when the global retention ratio for FLUTE was less than 0.62.<sup>20</sup> The global retention ratio of FLUTE was calculated based on the AD-related regions, including the frontal, parietal, lateral temporal, anterior, and posterior cingulate cortices.

#### *Statistical analyses*

The demographic and clinical characteristics of the study group were expressed as the means and standard deviation (SD). The Kolmogorov-Smirnov test was performed to check the normal distribution of variables in the AD and NC groups. The Mann-Whitney *U* test was used to determine the significance of the differences between the AD and NC groups for age, education years, and K-MMSE scores. For categorical variables (gender and ApoE ε4 carrier status), the chi-squared test was performed to compare the distribution between the AD and NC participants.

Voxel-wise comparisons of THK SUVR images of each group were performed in SPM12 (Statistical Parametric Mapping; Wellcome Trust Centre for Neuroimaging, London, UK) using a 2-sample *t*-test with adjustments for age, gender, and years of education. The results are presented at a threshold of *p*<0.001, uncorrected for multiple comparisons with adjustments for age, gender, and years of education, and a cluster >100.

The regional SUVR of the THK5351 was assessed using the Z score. Z scores were calculated for each voxel using the THK retention databases: Z score=[(THK retention in each bvFTD patient)-(mean value of NC group)]/normal SD. Regions with Z scores exceeding a threshold of *Z*>1.5 were classified as increased areas compared to the NC group.

## RESULTS

### **Study population**

Three patients with clinical and MRI features of bvFTD were enrolled. The demographics and clinical characteristics of the study population and the three patients with bvFTD are shown in **Table 1**. There were no statistically significant differences between age or gender between the NC (*n*=24) and AD (*n*=21) groups. The duration of education in the AD group was significantly shorter than in the NC group. Further, 57.1% of the AD group were ApoE ε4 carriers, but no one had ApoE ε4 in the bvFTD group.

**Table 1.** Demographic and clinical characteristics of the study population

Variables	NC	AD	p-value	bvFTD			Mean±SD
				Case 1	Case 2	Case 3	
No. of patients	24	21					
Age (yr)	73.96±4.72	76.33±6.07	0.178*	62	78	83	74.33±10.97
Sex (M:F)	11:13	7:14	0.393†	M	M	M	
Education (yr)	11.083±4.56	7.667±5.22	0.032*	12	12	6	10±3.46
Disease duration (mon)	-	65.76±28.48		60	36	24	40±13.85
K-MMSE	27.96±1.52	14.67±5.66	<0.001*	14	3	23	13.33±10.02
CDR-SB	0	7.5±2.34		14	18	4.5	12.17±6.93
ApoE ε4 carrier, No. (%)	4 (16.7)	12 (57.1)	0.011†	ε3/ε3	ε3/ε3	ε3/ε3	

Data are presented as the mean for non-normally distributed variables checked by the Kolmogorov-Smirnov test, and mean±SD not otherwise specified.

NC: normal cognition, AD: Alzheimer's disease, bvFTD: behavioral variant frontotemporal dementia, SD: standard deviation, M: male, F: female, K-MMSE: Korean version of the Mini-Mental State Examination, CDR-SB: Clinical Dementia Rating Sum of Boxes.

\*Mann-Whitney U test between the AD and NC groups; †χ<sup>2</sup> test between the AD and NC groups.

### Case summary

The first bvFTD patient was a 62-year-old male with 12 years of education who complained of abnormal behavioral and personality changes that began five years prior to his initial visit. His reckless driving had caused several traffic accidents and he had become an exhibitionist who often wandered around naked. His MMSE score was 14 and his CDR score was 2. Detailed neuropsychological test results showed poor performance in all cognitive domains. The NPI results showed that he had delusions, aggression, depression, anxiety, euphoria, disinhibition, irritability, abnormal repetitive behaviors, night-time behavior, and eating changes. Neurologic examination showed he had severe dysarthria, a reptile-like expression, drooling, a resting tremor in his left hand, rigidity (left > right), bradykinesia, gait disturbance, and postural instability. An MRI showed cortical atrophy in the bilateral frontal and anterior temporal cortices. <sup>18</sup>F-THK5351 retention was elevated in the bilateral frontal cortex, insula, and basal ganglia (right > left) (**Fig. 1A**). In regional analysis of the SUVR, high retention of the <sup>18</sup>F-THK5351 was observed in the prefrontal, medial temporal, anterior cingulate, amygdala, striatum, nucleus accumbens, dorsolateral prefrontal cortices, and brain stem, compared to the NC group. FLUTE PET showed amyloid negative.

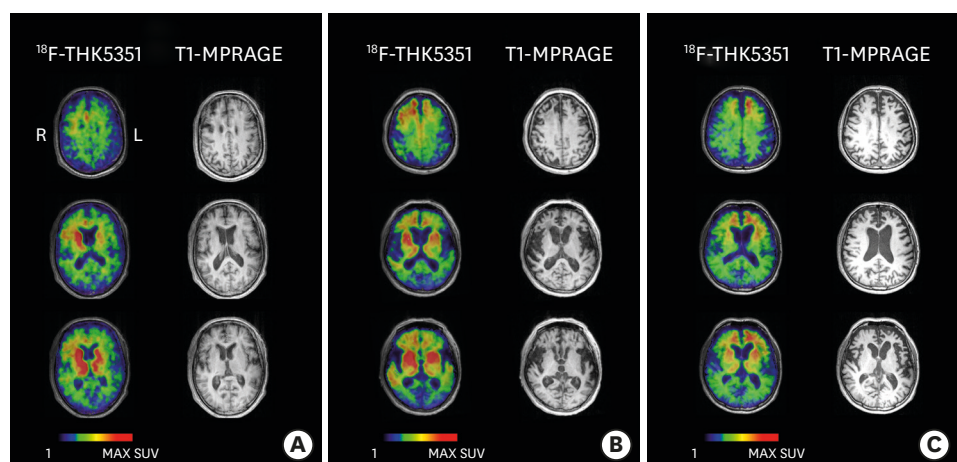


**Fig. 1.** <sup>18</sup>F-THK5351 PET SUV and magnetic resonance images of bvFTD patients.

Representative slices in the horizontal direction of <sup>18</sup>F-THK5351 PET and 3D T1-MPRAGE scans taken of three patients diagnosed with bvFTD.

PET: positron emission tomography, SUV: standardized uptake value, bvFTD: behavioral variant frontotemporal dementia, MPRAGE: magnetization-prepared rapid gradient-echo.

**Table 2.** Summary of 3 patients with bvFTD

Case number, sex/age (yr)	Disease duration (mon)	Presenting symptoms	NPI total score	MRI	<sup>18</sup> F-THK5351 PET	<sup>18</sup> F-Flutemetamol PET
1, M/62	60	Disinhibition, aggressive behavior, poor executive function, motor symptoms	29	Bilateral frontal and anterior temporal cortical atrophy	Bilateral frontal cortex, insula, and basal ganglia uptake	Amyloid negative
2, M/78	36	Aggressive behavior, apathy, disinhibition, irritability, memory complaints, poor executive function	32	Bilateral frontal and temporal cortical atrophy	Bilateral frontal, parietal, and temporal cortical uptake	Amyloid negative
3, M/83	24	Poor frontal, executive function, repetitive behaviors, wandering, eating changes, poor comprehension	14	Bilateral frontal and temporal cortical atrophy with diffuse brain atrophy	Medial/inferior frontal cortex and anterior temporal cortical uptake	Amyloid negative

bvFTD: behavioral variant frontotemporal dementia, NPI: neuropsychiatric inventory, MRI: magnetic resonance imaging, PET: positron emission tomography, M: male.

The second patient with bvFTD was a 78-year-old male with 12 years of education. He developed personality changes, abnormal behaviors, and memory decline three years prior to enrollment in the study. His MMSE score was 3 and CDR was 3. He failed to perform detailed neuropsychological tests. His NPI results revealed disturbances in agitation/aggression, apathy/indifference, disinhibition, aberrant motor behavior, sleep/night-time behavior, and eating behavior. The 3T MRI showed severe bilateral cortical atrophy in the frontal and temporal regions. <sup>18</sup>F-THK5351 retention was observed in the bilateral frontal, parietal, and temporal regions (right > left) (**Fig. 1B**). In regional SUVR, the prefrontal, inferior parietal, lateral and medial temporal, anterior and posterior cingulate, global cortex, orbital frontal, entorhinal, hippocampus, amygdala, superior, inferior, and middle temporal, striatum, nucleus accumbens, white matter, insula, medial frontal and dorsolateral prefrontal regions showed <sup>18</sup>F-THK5351 retention. FLUTE PET revealed negative for amyloid.

The third patient was an 83-year-old man with six years of schooling. He had rapidly developed an amnestic disorder within two years of the death of his partner. The patient displayed evident personality changes and abnormal behaviors, including irritability and swearing. His MMSE score was 23 and his CDR score was 1. The detailed neuropsychological test results indicated that he had poor performance in nearly all cognitive domains, except for visuo-spatial function. The NPI results indicated agitation, apathy, irritability, sleep problems, and appetite changes. The MRI showed diffuse brain atrophy, especially in the bilateral frontal and temporal cortices. He had significant <sup>18</sup>F-THK5351 retention in the medial and inferior frontal and anterior temporal cortices (**Fig. 1C**). In SUVR analysis, the patient showed high uptake in the prefrontal, lateral and medial temporal, anterior cingulate, global cortex, orbital frontal, entorhinal, hippocampus, amygdala, middle and inferior temporal, striatum, nucleus accumbens, white matter, insula, medial frontal, and dorsolateral prefrontal regions. FLUTE PET was negative for amyloid.

The clinical characteristics and imaging findings of each bvFTD patient are briefly summarized in **Table 2**, including presenting symptoms, neuropsychiatric findings, and imaging findings.

### Voxel-based analysis of <sup>18</sup>F-THK5351 retention in bvFTD, AD, and NC groups

Voxel-wise analyses of the <sup>18</sup>F-THK5351 PET scans are shown in **Fig. 2**. The bvFTD group showed higher bilateral retention in the medial frontal, dorsolateral prefrontal, orbitofrontal, anterior cingulate, insula, anterior inferior temporal, and striatum regions compared to the NC group. Left-right asymmetry was noted in the patients with bvFTD (**Fig. 2A**,

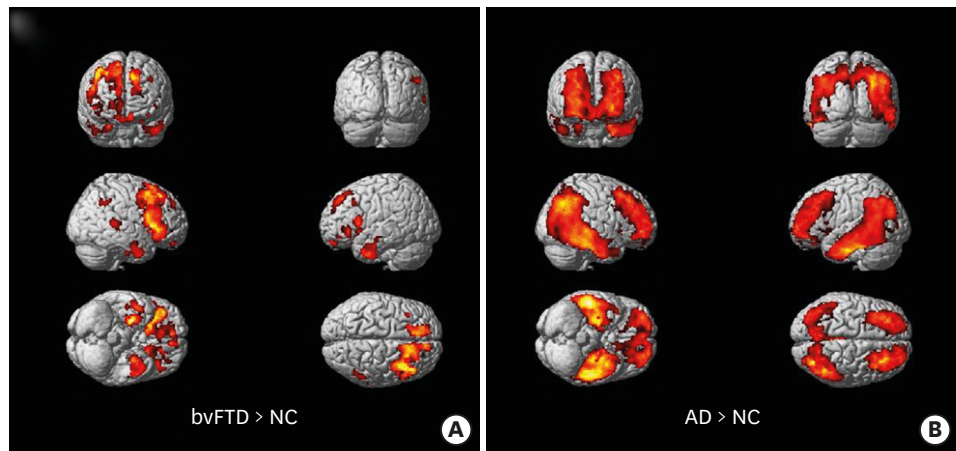


**Fig. 2.** Group comparison of  $^{18}\text{F}$ -THK5351 positron emission tomography. Colored areas represent brain regions corresponding to increased THK retention from voxel-wise statistical analyses in (A) the bvFTD group compared to the NC group (bvFTD > NC) and (B) the AD group compared to the NC group (AD > NC). The results are presented at a threshold of  $p < 0.001$ , adjusted for age, gender, and years of education, and a cluster  $> 100$ . bvFTD: behavioral variant frontotemporal dementia, NC: normal cognition, AD: Alzheimer's disease.

**Supplementary Fig. 1).** Meanwhile, the AD patients showed greater  $^{18}\text{F}$ -THK5351 retention in the bilateral medial and lateral temporal, and inferior parietal regions, dorsolateral prefrontal cortices, and the precuneus compared to the NC group (**Fig. 2B, Supplementary Fig. 2**).

Comparison of the bvFTD and AD groups showed that the bvFTD group had greater  $^{18}\text{F}$ -THK5351 retention in the inferior frontal cortices, anterior cingulate cortex, insula, and striatum regions (right > left). (**Supplementary Figs. 3 and 4**). There was no brain region showing AD group had greater THK retention than bvFTD.

#### ROI-based analysis of $^{18}\text{F}$ -THK5351 retention in bvFTD, AD, and NC groups

The ROI-based analysis, performed after partial volume correction, revealed higher  $^{18}\text{F}$ -THK5351 retention as a whole in the prefrontal, orbitofrontal, medial frontal, anterior cingulate, amygdala, and striatum regions in the bvFTD group (**Table 3**). The first case, with extrapyramidal symptoms, showed much greater  $^{18}\text{F}$ -THK5351 retention in the brainstem. In AD patients,  $^{18}\text{F}$ -THK5351 retention was significantly greater bilaterally in the frontal, parietal, temporal, occipital, precuneus, entorhinal, parahippocampus, and fusiform gyrus regions compared to NC group.

## DISCUSSION

In this study, we found that bvFTD patients showed increased retention of  $^{18}\text{F}$ -THK5351 in the medial frontal, dorsolateral prefrontal, orbitofrontal, anterior cingulate, insula, anterior inferior temporal regions, and striatum regions, compared to NC. The distribution of THK retention was consistent with cortical atrophy on the MRI images. Clinically, these areas highly-correlate with symptoms observed in bvFTD patients. The medial frontal cortex and anterior cingulate cortex are involved in social cognition, including representation of self, the perception of social groups,<sup>21</sup> and decision making.<sup>22</sup> The orbitofrontal cortex plays a role in personality and executive functions, as a part of an interactive functional system with a strong connection to the amygdala and other parts of the limbic system.<sup>23</sup> The inferior temporal cortex functions in semantic processing<sup>24</sup> and memory of visual patterns.<sup>25</sup> Meanwhile, the

**Table 3.** Regional SUVR of <sup>18</sup>F-THK5351 PET

Variables	NC (n=24)		AD (n=21)		bvFTD case 1		bvFTD case 2		bvFTD case 3	
	Mean (SD)	Mean (SD)	Mean (SD)	Z	Mean	Z	Mean	Z	Mean	Z
Prefrontal	1.66 (0.23)	2.18 (0.39)	2.25	2.25	2.10	1.83	4.00	10.12	2.99	5.72
Orbital frontal	2.20 (0.34)	2.70 (0.42)	1.49	2.25	0.13	5.50	9.75	5.50	9.77	
Medial frontal	1.58 (0.20)	1.95 (0.29)	1.67	1.88	1.37	4.09	11.51	2.71	5.16	
Dorsolateral prefrontal	1.49 (0.22)	2.28 (0.61)	3.51	1.90	1.81	3.40	8.49	2.12	2.78	
Medial temporal	2.77 (0.39)	4.19 (1.19)	3.63	3.39	1.60	5.80	7.72	4.04	3.24	
Superior temporal	1.90 (0.29)	2.28 (0.45)	1.30	1.56	-1.16	4.75	9.75	2.26	1.25	
Middle temporal	1.95 (0.29)	2.29 (0.45)	3.35	1.66	-1.02	4.21	7.88	3.09	3.97	
Inferior temporal	1.93 (0.28)	2.94 (0.63)	3.58	1.59	-1.20	2.68	2.64	2.58	2.31	
Superior parietal	1.41 (0.21)	1.94 (0.51)	2.50	0.85	-2.62	0.91	-2.36	1.13	-1.31	
Inferior parietal	1.59 (0.22)	2.36 (0.61)	3.44	1.51	-0.34	2.13	2.42	1.62	0.15	
Precuneus	1.73 (0.23)	2.59 (0.81)	3.67	1.86	0.58	1.74	0.04	1.71	-0.08	
Occipital	1.20 (0.18)	1.61 (0.39)	2.29	0.85	-2.02	0.51	-3.93	0.96	-1.35	
Anterior cingulate	3.24 (0.41)	3.40 (0.49)	0.40	4.59	3.28	5.72	6.02	4.64	3.40	
Posterior cingulate	2.19 (0.41)	2.80 (0.60)	1.49	1.89	-0.74	3.21	2.49	2.40	0.50	
Global cortex	1.75 (0.23)	2.36 (0.38)	2.69	1.83	0.34	2.99	5.43	2.45	2.17	
Sensorimotor	1.28 (0.19)	1.29 (0.30)	0.03	1.20	-0.45	1.16	-0.63	0.98	-1.58	
Entorhinal	2.42 (0.38)	4.37 (1.96)	5.15	2.56	0.36	7.90	14.50	4.26	4.87	
Hippocampus	2.74 (0.36)	3.99 (1.04)	3.47	3.04	0.83	4.92	6.05	3.73	2.76	
Amygdala	3.73 (0.63)	6.25 (2.39)	4.02	6.77	4.85	10.26	10.41	8.36	7.39	
Parahippocampus	2.25 (0.41)	6.25 (2.39)	1.63	2.12	-0.33	3.03	1.90	2.55	0.74	
Fusiform gyrus	1.80 (0.25)	2.51 (0.62)	2.79	1.45	-1.38	1.96	0.64	1.67	-0.53	
Lingual gyrus	1.37 (0.20)	1.59 (0.39)	1.15	0.81	-2.8	0.59	-3.92	1.00	-1.85	
Striatum	3.56 (0.51)	3.87 (0.67)	0.61	4.73	2.3	4.89	2.60	4.76	2.36	
Insula	2.42 (0.32)	2.84 (0.54)	1.29	2.63	0.62	5.08	8.15	4.33	5.86	
Brain stem	2.55 (0.25)	2.43 (0.31)	-0.46	3.73	4.8	2.74	0.77	2.54	-0.02	

Data are presented as mean and standard deviation for non-normally distributed variables. Z score=[(THK retention in each bvFTD patient)-(mean value of NC group)]/normal SD

SUVR: standardized uptake value ratio, PET: positron emission tomography, NC: normal cognition, AD: Alzheimer's disease, bvFTD = behavioral variant frontotemporal dementia, SD: standard deviation.

AD patients showed greater <sup>18</sup>F-THK5351 retention in the bilateral medial and lateral temporal, inferior parietal, dorsolateral prefrontal cortices, and precuneus regions compared to the NC group. Left-right asymmetry was noted in the bvFTD patients (right > left).

The pathologies of bvFTD have been known to be either TDP-43 or tauopathy, at nearly equal proportions.<sup>2-4</sup> Among tauopathies, Pick's disease (3R tauopathy) or PSP, and CBD (4R tauopathy) may present with bvFTD.<sup>26</sup> In this study, the first case, with disease duration of five years, had extrapyramidal symptoms and signs indicative of PSP or CBD. The underlying pathology of the other two cases could not be attributed to tauopathy or other pathologies. Although tau accounts for about half of the bvFTD cases, other pathologies, including TDP-43, fused in sarcoma proteins, the ubiquitin-proteasome system, and neuronal intermediate filaments have been shown to present as bvFTD. However, all three patients with bvFTD showed greater THK retention in the clinically-corresponding areas, and the regions with high THK retention were correlated with brain atrophy. A previous study indicated that the administration of MAO-B inhibitors reduced the uptake of <sup>18</sup>F-THK5351 throughout the entire brain, suggesting that the presence of MAO-B may confound the THK PET retention.<sup>11</sup> Elevated MAO-B levels have been associated with astrocytic degeneration<sup>27,28</sup> and neurodegenerative diseases, such as frontotemporal dementia. A recent paper reported that the THK5351 tracer detected not only neurofibrillary tangles, but a combination of neurofibrillary tangles and astrogliosis.<sup>29</sup> Neuroinflammation is known to progress throughout the disease course and correlates with tau burden, contributing to neurodegeneration.<sup>29,30</sup> Increased THK retention in all three bvFTD patients could be explained by astrogliosis related to neurodegeneration.

Our results agree with recent papers on tau PET findings in bvFTD,<sup>9,31,32</sup> although we did not show separate results for white and gray matter. Pathologic data has shown that most of the non-AD tauopathies exhibited tau pathology in the white matter as neuronal threads, global oligodendroglial inclusions, oligodendroglial coiled bodies, or thorn-shaped astrocytes. And a previous tau PET study showed that the brain regions where THK retention was increased were white matter.<sup>9,31</sup> Individual SUV mapping or group comparison may indicate that THK retention is greater in the white matter than in gray matter. However, due to the small number of patients in this study, we could not analyze white and gray matter separately. Our study suggests that <sup>18</sup>F-THK5351 PET imaging could be a supportive tool for diagnosis of bvFTD. Although the topographical distribution of THK retention might be clinically-beneficial to the diagnosis of bvFTD, issues regarding the ligand's non-specificity remain. Additionally, the small numbers of patients and lack of pathologic confirmation are major limitations of our study.

<sup>18</sup>F-THK5351 imaging has been known to reflect the combination of tau pathology and astrocytosis, which are associated with neurodegeneration,<sup>8</sup> and the THK retention sensitively reflects clinical symptoms in the corresponding brain areas. Therefore, <sup>18</sup>F-THK5351 topographical findings could be useful in differential diagnoses of bvFTD, AD dementia, and other dementia disorders. However, due to the non-specificity issue, the results may not provide information on the pathology (tauopathy, TDP-43, or other pathologies) of a bvFTD patient.

In conclusion, <sup>18</sup>F-THK5351 PET scans showed focal retention in the prefrontal, orbitofrontal, medial frontal, anterior cingulate, insula, amygdala, and striatum regions in bvFTD patients, which correlated with clinical symptoms and regional atrophy on the MRIs. However, due to the preliminary nature of this study, definite conclusions cannot be drawn about the nature of the target of such retentions. Further studies with a larger number of patients with a range of disease severities are needed to validate the clinical utility of <sup>18</sup>F-THK5351 PET for the diagnosis of bvFTD.

## SUPPLEMENTARY MATERIALS

### Supplementary Fig. 1

Behavioral variant frontotemporal dementia > normal cognition axial view (uncorrected  $p<0.001$ , adjustment for age, gender and years of education, cluster >100).

[Click here to view](#)

### Supplementary Fig. 2

Alzheimer's disease > normal cognition axial view (uncorrected  $p<0.001$ , adjustment for age, gender and years of education, cluster >100).

[Click here to view](#)

### Supplementary Fig. 3

Statistical parametric mapping analysis of <sup>18</sup>F-THK5351 standardized uptake value ratio images after partial volume correction between bvFTD and AD groups ( $p<0.001$ , uncorrected for multiple comparisons with adjustment for age, gender and years of education, a cluster >100).

[Click here to view](#)

**Supplementary Fig. 4**

Behavioral variant frontotemporal dementia > Alzheimer's disease axial view (uncorrected  $p<0.001$ , adjustment for age, gender and years of education, cluster >100).

[Click here to view](#)

**REFERENCES**

1. Mackenzie IR, Neumann M, Bigio EH, Cairns NJ, Alafuzoff I, Kril J, et al. Nomenclature and nosology for neuropathologic subtypes of frontotemporal lobar degeneration: an update. *Acta Neuropathol* 2010;119:1-4.  
[PUBMED](#) | [CROSSREF](#)
2. Mackenzie IR, Foti D, Woulfe J, Hurwitz TA. Atypical frontotemporal lobar degeneration with ubiquitin-positive, TDP-43-negative neuronal inclusions. *Brain* 2008;131:1282-1293.  
[PUBMED](#) | [CROSSREF](#)
3. Kertesz A, McMonagle P, Blair M, Davidson W, Munoz DG. The evolution and pathology of frontotemporal dementia. *Brain* 2005;128:1996-2005.  
[PUBMED](#) | [CROSSREF](#)
4. Rascovsky K, Hodges J, Knopman D, Mendez M, Kramer J, Neuhaus J, et al. Can clinical features predict tau pathology in patients with behavioral variant frontotemporal dementia (bvFTD)? *Neurology* 2013;80:P05.101.
5. Chare L, Hodges JR, Leyton CE, McGinley C, Tan RH, Kril JJ, et al. New criteria for frontotemporal dementia syndromes: clinical and pathological diagnostic implications. *J Neurol Neurosurg Psychiatry* 2014;85:865-870.  
[PUBMED](#) | [CROSSREF](#)
6. Dickson DW, Kouri N, Murray ME, Josephs KA. Neuropathology of frontotemporal lobar degeneration-tau (FTLD-tau). *J Mol Neurosci* 2011;45:384-389.  
[PUBMED](#) | [CROSSREF](#)
7. Chien DT, Szardenings AK, Bahri S, Walsh JC, Mu F, Xia C, et al. Early clinical PET imaging results with the novel PHF-tau radioligand [F18]-T808. *J Alzheimers Dis* 2014;38:171-184.  
[PUBMED](#) | [CROSSREF](#)
8. Harada R, Okamura N, Furumoto S, Furukawa K, Ishiki A, Tomita N, et al. 18F-THK5351: a novel PET radiotracer for imaging neurofibrillary pathology in Alzheimer disease. *J Nucl Med* 2016;57:208-214.  
[PUBMED](#) | [CROSSREF](#)
9. Cho H, Seo SW, Choi JY, Lee HS, Ryu YH, Lee MS, et al. Predominant subcortical accumulation of <sup>18</sup>F-flortaucipir binding in behavioral variant frontotemporal dementia. *Neurobiol Aging* 2018;66:112-121.  
[PUBMED](#) | [CROSSREF](#)
10. Lee MK, Hwang BY, Lee SA, Oh GJ, Choi WH, Hong SS, et al. 1-methyl-2-undecyl-4(1H)-quinolone as an irreversible and selective inhibitor of type B monoamine oxidase. *Chem Pharm Bull (Tokyo)* 2003;51:409-411.  
[PUBMED](#) | [CROSSREF](#)
11. Ng KP, Pascoal TA, Mathotaarachchi S, Therriault J, Kang MS, Shin M, et al. Monoamine oxidase B inhibitor, selegiline, reduces <sup>18</sup>F-THK5351 uptake in the human brain. *Alzheimers Res Ther* 2017;9:25.  
[PUBMED](#) | [CROSSREF](#)
12. Rascovsky K, Hodges JR, Knopman D, Mendez MF, Kramer JH, Neuhaus J, et al. Sensitivity of revised diagnostic criteria for the behavioural variant of frontotemporal dementia. *Brain* 2011;134:2456-2477.  
[PUBMED](#) | [CROSSREF](#)
13. McKhann G, Drachman D, Folstein M, Katzman R, Price D, Stadlan EM. Clinical diagnosis of Alzheimer's disease: report of the NINCDS-ADRDA Work Group under the auspices of Department of Health and Human Services Task Force on Alzheimer's disease. *Neurology* 1984;34:939-944.  
[PUBMED](#) | [CROSSREF](#)
14. Srikanth S, Nagaraja AV, Ratnavalli E. Neuropsychiatric symptoms in dementia-frequency, relationship to dementia severity and comparison in Alzheimer's disease, vascular dementia and frontotemporal dementia. *J Neurol Sci* 2005;236:43-48.  
[PUBMED](#) | [CROSSREF](#)
15. Greve DN, Svarer C, Fisher PM, Feng L, Hansen AE, Baare W, et al. Cortical surface-based analysis reduces bias and variance in kinetic modeling of brain PET data. *Neuroimage* 2014;92:225-236.  
[PUBMED](#) | [CROSSREF](#)

16. Greve DN, Salat DH, Bowen SL, Izquierdo-Garcia D, Schultz AP, Catana C, et al. Different partial volume correction methods lead to different conclusions: an (18)F-FDG-PET study of aging. *Neuroimage* 2016;132:334-343.  
[PUBMED](#) | [CROSSREF](#)
17. Ossenkoppele R, Schonhaut DR, Schöll M, Lockhart SN, Ayakta N, Baker SL, et al. Tau PET patterns mirror clinical and neuroanatomical variability in Alzheimer's disease. *Brain* 2016;139:1551-1567.  
[PUBMED](#) | [CROSSREF](#)
18. Okamura N, Furumoto S, Fodero-Tavoletti MT, Mulligan RS, Harada R, Yates P, et al. Non-invasive assessment of Alzheimer's disease neurofibrillary pathology using 18F-THK5105 PET. *Brain* 2014;137:1762-1771.  
[PUBMED](#) | [CROSSREF](#)
19. Lockhart SN, Baker SL, Okamura N, Furukawa K, Ishiki A, Furumoto S, et al. Dynamic PET measures of tau accumulation in cognitively normal older adults and Alzheimer's disease patients measured using [18F] THK-5351. *PLoS One* 2016;11:e0158460.  
[PUBMED](#) | [CROSSREF](#)
20. Thurfjell L, Lilja J, Lundqvist R, Buckley C, Smith A, Vandenbergh R, et al. Automated quantification of 18F-flutemetamol PET activity for categorizing scans as negative or positive for brain amyloid: concordance with visual image reads. *J Nucl Med* 2014;55:1623-1628.  
[PUBMED](#) | [CROSSREF](#)
21. Amadio DM, Frith CD. Meeting of minds: the medial frontal cortex and social cognition. *Nat Rev Neurosci* 2006;7:268-277.  
[PUBMED](#) | [CROSSREF](#)
22. Walton ME, Bannerman DM, Alterescu K, Rushworth MF. Functional specialization within medial frontal cortex of the anterior cingulate for evaluating effort-related decisions. *J Neurosci* 2003;23:6475-6479.  
[PUBMED](#) | [CROSSREF](#)
23. Happaney K, Zelazo PD, Stuss DT. Development of orbitofrontal function: current themes and future directions. *Brain Cogn* 2004;55:1-10.  
[PUBMED](#) | [CROSSREF](#)
24. Nobre AC, Allison T, McCarthy G. Word recognition in the human inferior temporal lobe. *Nature* 1994;372:260-263.  
[PUBMED](#) | [CROSSREF](#)
25. Visser M, Jeffries E, Lambon Ralph MA. Semantic processing in the anterior temporal lobes: a meta-analysis of the functional neuroimaging literature. *J Cogn Neurosci* 2010;22:1083-1094.  
[PUBMED](#) | [CROSSREF](#)
26. Burrell JR, Hodges JR, Rowe JB. Cognition in corticobasal syndrome and progressive supranuclear palsy: a review. *Mov Disord* 2014;29:684-693.  
[PUBMED](#) | [CROSSREF](#)
27. Sidoryk-Wegrzynowicz M, Wegrzynowicz M, Lee E, Bowman AB, Aschner M. Role of astrocytes in brain function and disease. *Toxicol Pathol* 2011;39:115-123.  
[PUBMED](#) | [CROSSREF](#)
28. Broe M, Kril J, Halliday GM. Astrocytic degeneration relates to the severity of disease in frontotemporal dementia. *Brain* 2004;127:2214-2220.  
[PUBMED](#) | [CROSSREF](#)
29. Harada R, Ishiki A, Kai H, Sato N, Furukawa K, Furumoto S, et al. Correlations of <sup>18</sup>F-THK5351 PET with postmortem burden of tau and astrogliosis in Alzheimer disease. *J Nucl Med* 2018;59:671-674.  
[PUBMED](#) | [CROSSREF](#)
30. Serrano-Pozo A, Mielke ML, Gómez-Isla T, Betensky RA, Growdon JH, Frosch MP, et al. Reactive glia not only associates with plaques but also parallels tangles in Alzheimer's disease. *Am J Pathol* 2011;179:1373-1384.  
[PUBMED](#) | [CROSSREF](#)
31. Son HJ, Oh JS, Roh JH, Seo SW, Oh M, Lee SJ, et al. Differences in gray and white matter (18)F-THK5351 uptake between behavioral-variant frontotemporal dementia and other dementias. *Eur J Nucl Med Mol Imaging* 2019;46:357-366.  
[PUBMED](#) | [CROSSREF](#)
32. Jang YK, Lyoo CH, Park S, Oh SJ, Cho H, Oh M, et al. Head to head comparison of [<sup>18</sup>F] AV-1451 and [<sup>18</sup>F] THK5351 for tau imaging in Alzheimer's disease and frontotemporal dementia. *Eur J Nucl Med Mol Imaging* 2018;45:432-442.  
[PUBMED](#) | [CROSSREF](#)